

Supporting Information

Biofuels from pyrolysis in perspective: trade-offs between energy yields and soil-carbon additions: *Dominic Woolf*^{*1}, *Johannes Lehmann*¹, *Elizabeth M. Fisher*², and *Largus T. Angenent*³

^{*1} College of Agriculture and Life Sciences, Cornell University, Ithaca NY 14850, USA. Phone 607 222 1730. Fax 607 255 2644. Email dw433@cornell.edu

² Sibley School of Mechanical and Aerospace Engineering, Cornell University, Ithaca NY 14850, USA

³ Biological and Environmental Engineering, Cornell University, Ithaca NY 14850, USA

Total number of Pages: 25
Total number of Figures: 6
Total number of Tables 3

Contents

Overview	2
1 Thermal processing of biomass	2
1.1 Yields from slow pyrolysis	2
1.2 Tar cracking	8
1.3 Gas cleanup	8
1.4 Heat and energy balance	9
1.4.1 Drying of biomass	9
1.4.2 Enthalpy of pyrolysis reaction	9
1.4.3 Combustion enthalpies of reactants and products	9
1.4.4 Heat losses	10
1.4.5 Parasitic power consumption	12
2 Pathways to fuels plus biochar	13
2.1 Gaseous fuels	13
2.1.1 Water gas -shift reaction for the production of hydrogen	13
2.1.2 Synthetic Natural Gas (SNG)	13
2.2 Liquid fuels	14
2.2.1 Methanol	14
2.2.2 Higher alcohols	15
2.2.3 Fischer-Tropsch alkanes	16
2.2.4 Bio-oils	18

Overview

This supporting information contains a detailed account of the assumptions used to model potential yields of fuels and biochar from pyrolysis, together with background information to justify these assumptions.

1 Thermal processing of biomass

1.1 Yields from slow pyrolysis

This section describes how we modelled the yields of solid (biochar), liquid (bio oil and water) and gaseous species (H_2 , CO , CO_2 , CH_4 , and light hydrocarbons). Yields of biochar, H_2 , CO , CH_4 , and light hydrocarbons were modelled by empirical regression equations derived from published values. Yields of CO_2 , bio oil and H_2O were then calculated to balance the C, H and O in reactants and products.

Yields of gaseous, volatile, and solid products of slow pyrolysis were modelled using a method based on that of Thunman et al.,¹ who used energy and elemental-mass balances, together with empirical relationships for yields of two species, to form a system of six simultaneous equations to solve for the yields of six volatile species. However, the model derived by Thunman et al.¹ was based on a narrow set of experimental data with a restricted range of validity.² Neves et al.,² therefore, sought to derive a similar model with broader applicability by using a more comprehensive dataset of published yields to solve for seven volatile species. However, Neves et al.² combined data for both fast and slow pyrolysis, resulting in a model that performs poorly for slow pyrolysis, predicting yields that differ significantly from reported measurements (and for some operating conditions predicting negative yields for some species).

We have, therefore, developed a detailed model of biomass slow pyrolysis that has the desired qualities of:

- (1) being based on a comprehensive metastudy dataset,
- (2) utilizing only slow-pyrolysis data,
- (3) predicting not just yields of main products (solid, liquid and gas), but also of the specific gas species evolved and the elemental compositions of the solid and liquid phases,
- (4) accounting for most of the variance in reported yields in terms of the main parameters that drive this variability (rather than simply assuming that variability is entirely unpredictable uncertainty), and
- (5) consisting of simple equations that are easy to apply to a wide range of feedstocks and pyrolysis conditions.

Absent such a model, most previous studies using models of biomass slow pyrolysis for techno-economic or lifecycle assessment have relied upon simplistic models derived from small datasets that only predict main products (see, for example, ³⁻⁸). Here we have sought to address this gap by developing a simple empirical model of yields and compositions based on an extensive survey of published data specifically for slow pyrolysis.

Empirical regression equations for the yield (as a function of temperature) for four species (CO , H_2 , CH_4 and C_2H_x hydrocarbons), were derived using data from ⁹⁻¹⁶. The forms of the regression equations were selected to represent the main features of the gaseous yield-temperature

responses, i.e. at lower temperatures (below 300-400 °C) gas species yields are very low; while above 400 °C gas yield rises rapidly. But yields of gaseous species do not rise indefinitely with temperature, but, rather, plateau at high temperatures as the pyrolysis reaction approaches completion and equilibrium concentrations of evolved gases are approached.¹⁷ Sigmoidal functions were therefore used to represent this temperature trend of negligible yield, followed by increasing yield, followed by plateau. The type of sigmoid functions are Weibull CDF curves, which are preferable to the logistic function here, because they allow for an asymmetry between how rapidly the slope increases at low temperatures and how rapidly it tends towards its asymptote at high temperatures. In the case of CO, an additional mid-range (400-550°C) plateau in yield is strongly evident in the empirical data, and a double sigmoidal form was therefore selected to represent this. The empirical equations, were calculated using the nls() non-linear least-squares-optimization function in the R statistical programming language, and are shown below (Eq. 1-4), and are plotted together with the measured data in Fig. S1, panels a-d.

$$Y_{\text{co}} = \frac{0.043}{1+\exp(17.2-0.03T)} + \frac{0.317}{1+\exp(10.9-0.01T)} \quad (\text{RSE} = 0.03) \quad (1)$$

$$Y_{\text{h2}} = 2.95\text{e-}2*(1-\exp(-3.50\text{e-}3*T))^{62.98} \quad (\text{RSE} = 0.002) \quad (2)$$

$$Y_{\text{ch4}} = 7.82\text{e-}2*(1-\exp(-3.38\text{e-}3*T))^{30.15} \quad (\text{RSE} = 0.004) \quad (3)$$

$$Y_{\text{c2hx}} = 3.6\text{e-}2*(1-\exp(-5.22\text{e-}3*T))^{154.97} \quad (\text{RSE} = 0.006) \quad (4)$$

where, T is the peak pyrolysis temperature (K), and RSE = residual standard error.

An empirical equation for dry, ash-free (DAF) biochar yield was also derived from published values for slow pyrolysis.^{9,10,12,18-32} These biochar yield data are shown, categorised by feedstock, in Fig. S2. A preliminary multiple regression was performed on these data using pyrolysis temperature, and feedstock composition (lignin, cellulose, hemicellulose, C, H, O and ash content) as model predictors. Where given, published values for biomass composition were used. Where these were not available from the published article, mean values for each biomass type were taken from the Phyllis database of biomass properties.³³ Multiple regression showed that temperature and feedstock-lignin content were the most important predictors of biochar yield, accounting for 50% and 30% of R², respectively (using the Proportional Marginal Variance Decomposition (pmvd) method of regressor relative importance in the Relaimpo library for the R statistical programming language, with 95% bootstrap confidence intervals). We therefore derived an empirical regression model for biochar yield (Y_ch) as a function of pyrolysis temperature T (K) and feedstock lignin mass fraction (L_f) (Eq. 5), shown plotted together with the measured data in Fig. S1, panel g.

$$Y_{\text{ch}} = 0.126 + 0.273*L_{\text{f}} + 0.539*\exp(-0.004*T) \quad (\text{R}^2=0.65) \quad (5)$$

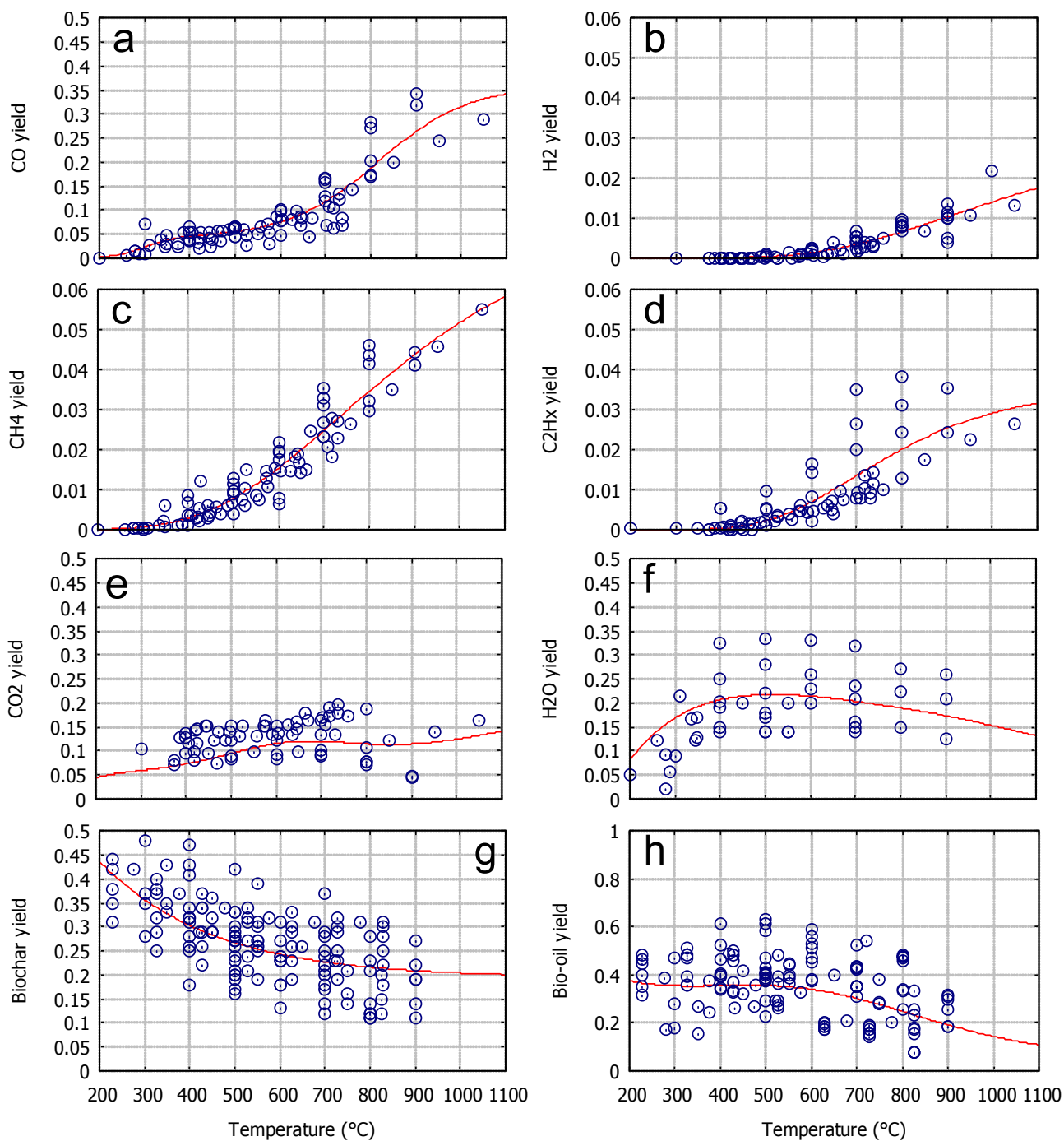


Fig. S1: Yields of gaseous, volatile and solid products of slow pyrolysis as a function of maximum pyrolysis temperature. Panels a-d show regressions of published empirical data for gaseous species (Eq. 1-4). Panel g (biochar yield) shows the regression of published data (Eq. 5), for a biomass lignin fraction of 0.25, with experimental data corresponding to lignin fractions between 9.2% and 59%. Panels e, f and h (CO₂, H₂O and bio-oil) are derived by balancing the elemental compositions of reactants and products according to Eq. 6-12 (for biomass of 50% C, 6% H, and 42% O, on DAF basis). Blue circles show empirical data.³⁻²⁵

The remaining variance in pyrolysis yields unexplained by this regression model is attributable to the wide variety of feedstocks and process conditions employed in this diverse set of studies. Solid, gaseous and volatile yields of pyrolysis are affected not only by the feedstock's lignin content, but also by its cellulose and hemicellulose content,^{17,20,34-36} ash content,³⁶⁻³⁸ particle size,³⁹⁻⁴³ initial moisture content,^{44,45} and by process conditions other than maximum temperature such as heating rate, pressure and gas residence time.^{17,46,47}

For the elemental (C, H, and O) composition of biochar (DAF basis), the empirical relations suggested by Neves,² which showed no significant difference between values for fast or slow pyrolysis, were used (Eq. 6-8). Bio-oil from slow pyrolysis, however, is considerably less oxygenated than fast-pyrolysis oil and shows no significant correlation with temperature,² therefore, its composition was described by Equations 9-11 derived from references^{10,19,21,22,24,30-32,48}.

$$Yc_ch = 0.93 - 0.92 \cdot \exp(-0.42e-2 \cdot T), \quad (R^2 = 0.65) \quad (6)$$

$$Yh_ch = -0.0041 + 0.1 \cdot \exp(-0.24e-2 \cdot T), \quad (R^2 = 0.75) \quad (7)$$

$$Yo_ch = 0.07 + 0.85 \cdot \exp(-0.48e-2 \cdot T), \quad (R^2 = 0.56) \quad (8)$$

$$Yc_tar = 1.25 Yc_f, \quad (R^2 = 0.83) \quad (9)$$

$$Yh_tar = 1.25 Yh_f, \quad (R^2 = 0.80) \quad (10)$$

$$Yo_tar = 1.17 Yo_f - 0.21. \quad (R^2 = 0.71) \quad (11)$$

where Yx_ch , Yx_tar and Yx_f ($x \in \{c,h,o\}$) are the mass fractions of C, H and O in the DAF biochar, tar (bio-oil) and feedstock, respectively.

The results presented in the main manuscript assume a feedstock of 50% C, 6% H and 43% O and 25% lignin, on a DAF basis. Note that the biochar yield may vary from values predicted from these parameters by up to +/- 0.09 (1 s.d), with a corresponding variation in the combined yield of fuel products (bio-oil and gas) of +/- 0.09.

The remaining unknown yields of bio-oil ($Ytar$), CO_2 ($Yco2$), and H_2O ($Yh2o$) are then calculated by solving Eq. 12 to balance the C, H, and O in reactants and products.

$$\begin{pmatrix} Yc_tar & Yc_co2 & 0 \\ Yo_tar & Yo_co2 & Yo_h2o \\ Yh_tar & 0 & Yh_h2o \end{pmatrix} \begin{pmatrix} Ytar \\ Yco2 \\ Yh2o \end{pmatrix} = \begin{pmatrix} Uc \\ Uo \\ Uh \end{pmatrix}, \quad (12)$$

where Uc , Uo , and Uh are the C, H, and O, respectively, that are unaccounted for in the already-calculated yields of biochar, CO , H_2 , CH_4 , and C_2H_x (which is approximated as C_2H_2).

Uncertainty and sensitivity analysis

We already have estimates of uncertainty in Eq.s 1 to 11 for those yields (biochar, CO , H_2 , CH_4 , C_2H_x , Yx_ch , and Yx_tar) that are directly calculated by regression. However, the uncertainties in those yields (bio-oil, CO_2 , and H_2O) calculated by Eq.12 remain to be quantified, and may be sensitive to the uncertainties in the input parameters to Eq. 12. Sensitivities of bio-oil, CO_2 , and H_2O yields to each of their model parameters are shown in Fig. S3. These sensitivities show the range of variation in yield (expressed as a percentage change relative to its mean value) as each parameter is varied by +/- 1 standard deviation from its mean value. We note that the variances of H_2 , CO , CH_4 and C_2H_x yields show a strong temperature dependence. Therefore, we estimated the variance of these parameters as a function of temperature by linear regression of the natural logarithm of the squares of the residuals. The sensitivities of bio-oil, CO_2 , and H_2O are then shown in Fig. S3 for three representative temperature points (450, 700, and 950 °C).

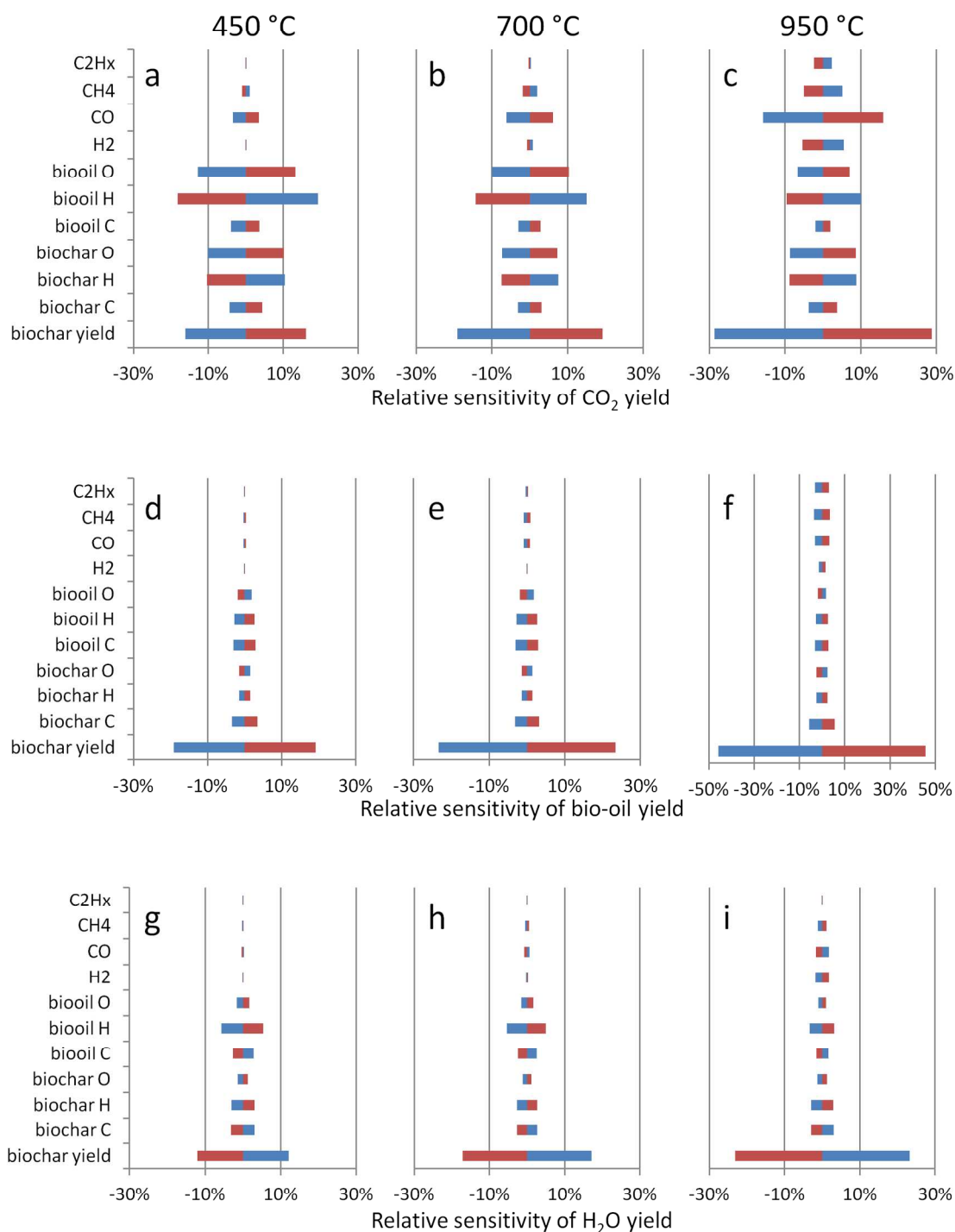


Fig. S3: Sensitivity of CO_2 , bio-oil, and H_2O yields (i.e., those product yields calculated by Eq. 12) to predicted yields (of C_2H_x , CH_4 , CO , H_2 , and biochar) and compositions (of biochar and biooil) of the other products of pyrolysis. Sensitivities are shown at three temperatures: 450 °C (left column), 700 °C (center column), and 950 °C (right column). In each case, the sensitivity is expressed as a percentage change in the product yield (relative to its mean value) as each parameter is varied by ± 1 standard deviation from its mean value. Mean values for the yield are given in Table S1. Blue bars indicate change in product yield with increasing parameter value. Conversely, red bars indicate change in product yield with decreasing parameter value.

Finally, a multivariate (Monte Carlo, $n = 10,000$) sensitivity analysis was used to estimate the standard deviation (s.d.) of bio-oil, CO_2 , and H_2O yields at the same three representative temperature points (Table S1).

Table S 1: Estimated uncertainties in yields of bio-oil, CO_2 , and H_2O . Standard deviation (s.d.) is estimated by Monte Carlo analysis ($n=10,000$).

	450 °C		700 °C		950 °C	
	Mean	s.d.	mean	s.d.	mean	s.d.
CO₂	0.093	0.04	0.11	0.04	0.083	0.047
Bio-oil	0.36	0.06	0.30	0.06	0.16	0.06
H₂O	0.21	0.03	0.20	0.04	0.17	0.04

1.2 Tar cracking

The impact of tar cracking on product yields was calculated by assuming that catalytic activity (catalytic cracking) or temperature (thermal cracking) is sufficient to bring the products to their equilibrium composition. The input stream to the equilibrium calculation consisted of the gases, bio-oil, water from pyrolysis, and water from moisture content of the original biomass. Bio-oil was described as a generic compound of formula $\text{C}_x\text{H}_y\text{O}_z$, with x , y , and z calculated from the bio-oil elemental composition (Eqs 9-11). For the results given in the main manuscript, moisture content of the original biomass was assumed to be 15%, and catalytic cracking at 800 °C, 1 bar was assumed. Equilibrium compositions were calculated using the NASA-developed software program *Chemical Equilibrium with Applications* (CEA).⁴⁹

1.3 Gas cleanup

In addition to removal of tars from the pyrolysis gases, removal of entrained particulates (principally char and ash) is typically also necessary, with the extent of gas cleanup required depending upon the nature of the downstream processes that utilise the gas. Some methods of gas cleanup, such as wet scrubbing or cold filtration, require that the gas stream be cooled to near ambient conditions. However, when the downstream process requires high temperatures, then cooling the syngas to perform scrubbing, followed by reheating the syngas would greatly reduce the overall thermal efficiency of the process. In such cases, therefore, some form of hot gas conditioning using a combination of a cyclone to remove larger particles followed by hot filtration (using, for example, ceramic/metallic candle filters) to remove finer particulates, together with tar-cracking conditions designed to produce very low levels of residual volatiles may be the preferred method. For the purpose of calculating the process energy balance in this study, it was assumed that there would be no cooling and subsequent reheating of gas streams.

In practice, achieving sufficient gas cleanup for those conversion pathways that require high purity gas streams may be one of the most challenging aspects of biomass conversion. However, for the purposes of comparing the mass and energy balances achievable through different pathways, it was simply assumed that sufficient cleanup would be possible, with a full system design specifying how this would be achieved being outside the scope of this study.

1.4 Heat and energy balance

1.4.1 Drying of biomass

Energy required for drying of biomass was calculated as the difference between the energy required to raise water at s.t.p. (20 °C, 1 atm) to steam at the pyrolysis or tar-cracking temperature (at 1 atm), minus any heat recovered (see Section 1.4.4) from the steam. The results presented in the main manuscript assume a biomass moisture content of 15%.

1.4.2 Enthalpy of pyrolysis reaction

Pyrolysis of biomass comprises both exothermic and endothermic processes, with tar formation and volatilisation being predominantly endothermic and char formation being exothermic.¹⁷ Overall, the net enthalpy change of the pyrolysis chemical reactions (ΔH_{py}) may be positive or negative, depending both on feedstock characteristics (with higher lignin content giving rise to greater char formation and a larger exothermic contribution) and also on process conditions, with factors that encourage greater char yield (such as increased residence time or pressure) also giving a more exothermic or less endothermic reaction.⁴⁶ Here, rather than assume any particular value for enthalpy of reaction, we calculate the enthalpy in product streams using the yields of individual components calculated according to 1.1-1.2 above. From the 1st Law of thermodynamics, we know that the energy input to the pyrolysis / tar-cracking system is equal to the energy out (Eq. 13).

$$\Delta H_{c_bm} + Q_f = \Delta H_{c_prod} + Q_{ex} + Q_l, \quad (13)$$

where,

ΔH_{c_bm} = heat of combustion of the biomass,

ΔH_{c_prod} = the combined heat of combustion of the gaseous, volatile and biochar products,

Q_f = heat supplied from fuel,

Q_{ex} = heat remaining in products at the temperature they exit the system after any heat recovery,

Q_l = heat lost from walls of the apparatus.

ΔH_{c_bm} and ΔH_{c_prod} were calculated as in Section 1.4.3 below. The heat losses Q_{ex} and Q_l were calculated as in Section 1.4.4 below. Thus, the only remaining unknown in Eq. 13, Q_f , can be calculated.

1.4.3 Combustion enthalpies of reactants and products

During steady state, the total energy entering the system (biomass + air enthalpy) is equal to the energy leaving the system (total enthalpy in the biochar, volatiles and gases, plus heat losses). Thus, when combustion of pyrolysis gases or volatile products provides the process heat and parasitic power requirements, the fraction of the initial energy content of the biomass that is available for use after pyrolysis and tar-cracking depends on two factors: 1) the energy remaining in the biochar and 2) the energy lost (either directly as heat from the thermal processing or as heat from parasitic power consumption).

The energy content of the biochar can be calculated from the yield of biochar (Eq. 5) and its heating value (Eq.s 6-8, 13). The higher heating values (HHV) of the biomass, biochar (on a dry, ash-free basis) and volatiles were calculated according to the Channiwala-Parikh equation,⁵⁰ assuming contributions to the HHV from N and S are negligible (Eq. 14):

$$\text{HHV (MJ kg}^{-1}\text{)} = 34.91 \text{ C} + 117.83 \text{ H} - 10.34 \text{ O} \quad (14)$$

The enthalpy of combustion remaining in the biochar ($\Delta H_{c_{ch}}$) is thus found to fall from 9 GJ Mg⁻¹ feedstock for pyrolysis at 300 °C, asymptotically approaching 6.5 GJ Mg⁻¹ feedstock for pyrolysis at >800 °C (Fig. S4).

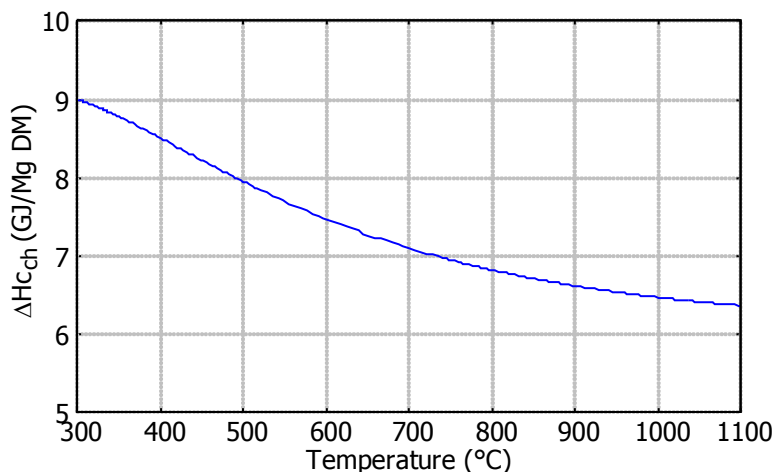


Fig. S4: Combustion enthalpy ($\Delta H_{c_{ch}}$), on a higher heating value basis, in biochar as a function of pyrolysis temperature, expressed relative to unit mass of dry feedstock.

The enthalpy of combustion of the gas was calculated from the heating values of the component gases, assuming HHVs (in GJ Mg⁻¹) of 141.8 (H₂), 10.1 (CO), 55.5 (CH₄), 51.9 (C₂H₆), 50.33 (C₂H₄), and 49.97 (C₂H₂).

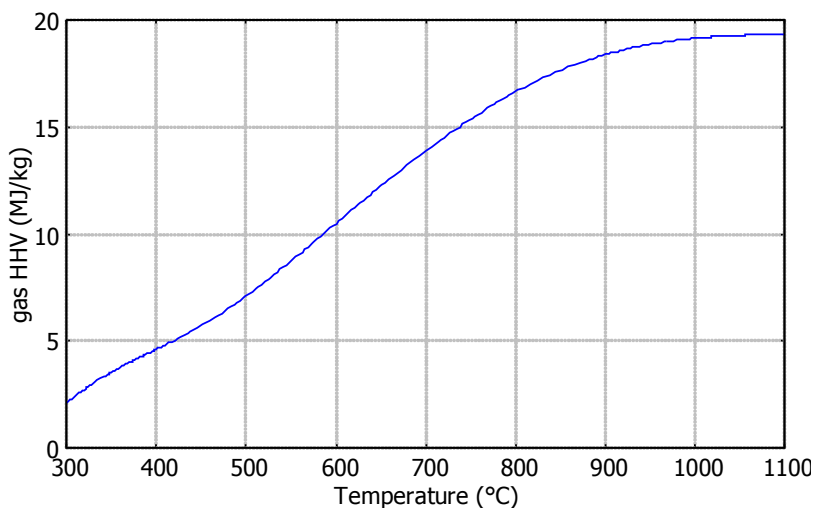


Fig. S5: Higher heating value (HHV) of pyrolysis gas, as a function of pyrolysis temperature.

1.4.4 Heat losses

The net heat losses comprise heat loss from the walls of the apparatus (Q_l), combined with sensible and latent heat in the volatiles (including steam), gases, and biochar, following any heat recovery (Q_{ex}) (Fig. 1, main manuscript; Eq. 13). Heat losses from energy used to provide motive power for prime movers (this includes heat produced during energy conversion to supply this power and also heat dissipated from those power loads themselves) also need to be accounted for

and are considered in Section 1.4.5. Energy for process heat and power can be provided using a range of possible fuel sources. The effects of using syngas, bio-oil, biochar, or additional biomass to provide process heat and power were each investigated.

Heat loss from the pyrolysis retort was estimated by assuming that the pyrolysis vessel was a cylinder with a length:radius aspect ratio of 20 encased in a 25-mm thick layer of calcium silicate insulation with a thermal conductivity of $0.123 \text{ W m}^{-1} \text{ K}^{-1}$. The volume of the cylinder (V) was calculated as $V = \dot{M}_w \frac{t_r}{\rho_b}$, where \dot{M}_w is the feed rate of wet biomass, t_r is the residence time of the biomass in the reactor and ρ_b is the bulk density of the feedstock (including any free space in the reactor). The residence time required for the carbonisation reaction to proceed to near-completion depends primarily on the pyrolysis temperature, and the thermal properties (heat capacity and heat transfer coefficients) of the biomass fragments. To a close approximation, the time required for pyrolysis depends upon which of the following three processes is rate-limiting: reaction kinetics, heat transfer to the biomass-particle surface, or internal heat transfer within the biomass particles.⁵¹ The question which of these processes dominates largely depends on the particle size.⁵² For this study, the conservative assumption was made that thermally thick particles would be used, with the conversion time calculated according to the values given by Di Blasi⁵² for a particle half-thickness of 20 mm (at which size the conversion time varies from 50 min at 700K to 20 min at 1100K). No additional heat loss from the walls of the tar-cracker was assumed, because, in a thermally-integrated design, heat from a tar-cracker operating at a higher temperature than the pyrolysis could be dissipated directly into the pyrolysis chamber (e.g. by siting the tar-cracker within the pyrolyser or within the gas stream that heats the pyrolyser).

Further heat losses may occur from the cooling of product streams exiting the pyrolysis/cracking reactor. How large these heat losses are depends on the non-chemical enthalpy in the product streams (including both sensible and latent heat) and on how much of this enthalpy is recovered. Table S2 gives the values of heat capacity at constant pressure (C_p) and enthalpy of vaporization (ΔH_v) values used. Enthalpy in steam was calculated using NIST formulae.⁵³ It was assumed that none of the sensible heat of the biochar would be recovered. How much heat might be recovered from the volatile and gaseous product streams depends on the downstream processes for which they will be used. It was assumed that any cooling of the pyrolysis gas or syngas required prior to downstream processing would be achieved with heat recovery (for example, to provide energy for pre-heating and drying of incoming biomass feedstock), subject to the condition that in no case would the gases be cooled so far as to cause condensation of tar within the heat-recovery heat-exchangers to become problematic. The dew-point of tars is highly variable depending on their composition, with higher molecular weight tars condensing at higher temperatures. This means that there is no precisely defined cut-off temperature below which tars will not condense. Rather, there is a relationship between the condensation temperature and the fraction of the tars that will condense, with higher temperatures leading to slower rates of tar deposition (and thus, a lower frequency required for cleaning operations). The lower limit on heat-recovery temperature was set at 350°C for systems without tar-cracking and 170°C for systems that include a tar-cracker, below which temperatures condensation of tar is likely to cause excessive problems.⁵⁴ For pyrolysis gases produced at temperatures below this, no heat recovery was assumed.

	Cp (J/g K)	ΔH_v (MJ/kg)	reference
CO ₂	0.844		55
CO	1.02		55
C ₂ H ₄	1.53		55
CH ₄	2.22		55
H ₂	14.32		55
biochar	0.8		56
bio-oil	3.0	1.22	57

Table S2: Values used for heat capacity at constant pressure (Cp) and heat of vaporization (ΔH_v) for products of pyrolysis.

1.4.5 Parasitic power consumption

Parasitic power consumption in slow-pyrolysis plants is typically lower than for fast pyrolysis for two reasons: 1) the feedstock does not need to be finely ground⁵⁸ and 2) the feed system in a slow-pyrolysis system is typically a slowly rotating worm gear with little friction compared to the much more rapidly rotating parts and/or fluidised beds required for fast pyrolysis⁵⁹. Mechanical power (which is typically supplied electrically) will nonetheless be required for operations such as: (1) transport within the pyrolysis reactor with a screw conveyer or other mechanical device. (2) comminution and transport of incoming feedstock. (3) maintaining a pressure drop through gas-cleaning apparatus such as cyclones and filters. (4) pumping air feed to combustors providing process heat. Overall, the power consumption for slow pyrolysis has been estimated to be 72 MJ Mg⁻¹,⁵⁹ considerably lower than the 170 MJ Mg⁻¹ estimated for fast pyrolysis.⁵⁸ A further 530 MJ Mg⁻¹ was allowed for comminution (based on chipping of woody feedstock,⁶⁰ although this requirement would vary considerably between feedstocks). It was assumed that this mechanical power would be provided by integrated power generation using the same fuel source utilised to provide process heat, at a conversion efficiency of 35%.

2 Pathways to fuels plus biochar

2.1 Gaseous fuels

2.1.1 Water gas -shift reaction for the production of hydrogen

For fuel pathways that require a syngas with a higher H₂ to CO ratio than is formed during pyrolysis or tar-cracking, the H₂ content may be increased by reacting CO with H₂O in the water gas-shift (WGS) reaction (Eq. 15), which produces one mole of H₂ for each mole of CO consumed.



The WGS reaction is a slightly exothermic ($\Delta H^\circ = -41 \text{ kJ mol}^{-1}$), reversible reaction typically performed at between 190-350 °C in the presence of a catalyst. Higher temperatures give greater reaction rates, but shift the equilibrium further to the left-hand-side reactants. In contrast, lower temperatures favour a higher conversion to H₂ albeit at a lower rate. Industrial applications often utilize a two-stage reactor to achieve both high reaction rates and high H₂ yields, with the first stage using an iron oxide / chromium oxide catalyst at around 350 °C, followed by a zinc oxide / aluminium oxide catalyst at 190–210 °C.

H₂ has itself been considered as a transport fuel, often in conjunction with fuel-cell vehicles.⁶¹ However, technical and economic issues with transport and storage of H₂ make it unclear whether this will emerge as an economically feasible form of transport infrastructure.⁶² H₂ can also be utilised as a reactant for the production of other types of gaseous fuels, such as CH₄, liquid fuels, including alcohols and alkanes, and for the upgrading of bio-oil. Where H₂ is required as a reactant, rather than as a fuel in its own right, the role of WGS would be not to shift all CO to H₂, but to provide the desired H₂:CO ratio for downstream reactions. Therefore, a single-stage reaction with higher temperatures, and consequently higher reaction rates (with associated lower capital costs), would be more practical than when a complete shift to H₂ is desired.

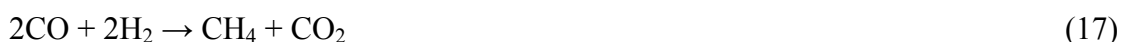
2.1.2 Synthetic Natural Gas (SNG)

SNG refers to a manufactured gas that resembles natural gas in having a high concentration of CH₄, together with small quantities of other light hydrocarbons, sometimes also with small amounts of other gases such as CO₂ or CO. There are a few routes to the conversion of biomass to SNG together with biochar. Firstly, SNG can be produced from biomass by anaerobic digestion (AD), a process that generates biogas (a mixture of mostly CH₄ and CO₂) from an anoxic slurry of biomass and water by the action of a microbial community containing methanogens. Yield of CH₄ varies with feedstock, with higher lignin and cellulose contents giving rise to less CH₄. For lignocellulosic feedstocks such as straw, CH₄ yield is around 5.6-8.5 GJ Mg⁻¹ DM (the mean of 7.1 GJ, equivalent to 7.7 GJ Mg⁻¹ DAF, was assumed for this study).⁶³ Approximately 30% of the biogas produced is required to provide heat and power to the digester.⁶³ Raw biogas is typically 50-70% CH₄.⁶⁴ Biogas can be upgraded to SNG with > 90% CH₄, suitable for use as a fuel, by removal of CO₂ (and trace quantities of H₂S) by absorption in water, organic solvents or internally in digester sludge, by pressure-swing adsorption, or by membrane separation.⁶⁵ Upgrading typically requires around 11% of the energy in the biogas.⁶³ Accounting for energy required for AD and biogas-upgrading, the overall yield of SNG is thus approximately 4.7 GJ Mg⁻¹ DAF. Although AD does not itself generate biochar, it does yield approximately 0.5 Mg DM Mg⁻¹ DM of residue that could be used as a feedstock for pyrolysis,

consisting of less-readily digested (lignin-rich) biomass and lysed cells. In conventional AD, the digestate is approximately 90% water. In so-called dry AD, the digestate water content may be reduced to around 60-80%,⁶⁶ but is still high for use as a pyrolysis feedstock. Dewatering by pressing and/or centrifuging can reduce the water content to around 35-50%.⁶⁷ Nonetheless, at this high water content, pyrolysis would not be able to co-produce significant additional energy (beyond the SNG derived from the AD stage) due to the high energy requirement for drying the feedstock. At best, it could be self-sufficient in energy.

The second method for coproduction of biochar and SNG is simply to capture the CH₄ and light hydrocarbons produced in the pyrolysis gases and separate them from other diluents.

A third potential method of SNG production is by catalytic methanation of syngas (Eqs. 16-18). Catalytic methanation is currently used commercially, not for CH₄ production, but in NH₃ production to remove the last remaining carbon oxides from syngas-derived hydrogen, because they would poison the ammonia-synthesis catalysts. However, in the late 1970's and 1980's, when it was widely believed that natural gas reserves were vulnerable to rapid depletion or geopolitical restriction, there was also considerable interest in methanation of syngas to produce SNG from coal.⁶⁸ With the discovery of widespread gas reserves over the last two decades and the increasing, but contentious, development of shale-gas resources, the perceived role of SNG for near-term energy security has dwindled. Nonetheless, catalytic methanation of biomass-derived syngas could also provide a means to produce renewable SNG both as a climate-change mitigation strategy and to provide CH₄ fuel in geographic regions with biomass resources but where natural gas availability is limited.



Methanation is highly exothermic and is typically conducted at between 300-450°C and 30-70 bar.⁶⁹ Overall energy efficiencies from feedstock to SNG (taking account of all system components including gas conditioning and SNG upgrading) of up to 67% (on an HHV basis) are achievable using allothermal gasifiers that produce 10% CH₄ in the syngas, with the syngas to SNG stages having a net energy efficiency of 83%.⁷⁰ For gasifiers that produce a hydrocarbon-free syngas, the typical syngas to SNG conversion energy efficiency is 81%.⁷⁰ It was assumed here that the syngas would be produced using a tar-cracking catalyst that does not reform the CH₄ content of the pyrolysis gas and that the H₂:CO ratio would be shifted by WGS to the optimal value of 3:1 prior to methanation, with the H₂ and CO being methanated at a net energy efficiency of 81% (HHV).

2.2 Liquid fuels

2.2.1 Methanol

Methanol has been widely discussed as a transport fuel, which can be used in current internal combustion engines with only minor modifications.⁷¹ The traditional method of methanol synthesis from the early 19th until the early 20th century was by “destructive distillation” of wood, a process in which pyrolysis is combined with a fractionation column to separate economically valued products including methanol, turpentine, terpenes, tar and acetic acid. Yields of methanol by this process are generally small (1.0% by DAF weight from softwood, 1.7% from hardwood), although some feedstocks (7.8% from hazelnut shells) can give better yields.⁷²

More recently, catalytic methanol synthesis from syngas (Eqs. 18-19) has become the dominant method of methanol production worldwide.



The most widely used catalyst is a Cu/ZnO/Al₂O₃ composite developed by ICI in the 1960's, operating at 250-280°C and 50-80 bar. Prior to this development, existing catalysts had much lower activity, requiring that they be operated at much higher pressures of 100-200 bar. Modern low-pressure methanol-synthesis catalysts are, however, highly prone to sulphur poisoning, requiring syngas S to be reduced to below at least 0.5ppm and preferably below 0.1ppm in order to maintain catalyst life.⁷³ Syngas for commercial methanol production is predominantly made by steam reforming of methane (Eq. 21), which yields a mixture too rich in H₂ to produce methanol by the reaction in Eq. 19. Therefore, CO₂ is often added to the mixture to utilise the excess H₂ by the reaction in Eq. 20. Syngas derived from biomass pyrolysis, on the other hand, generally has a H₂:CO ratio less than or equal to the optimal 2:1 for methanol synthesis. It was assumed for this study that, where necessary, WGS would be used to adjust the H₂:CO ratio to 2:1 prior to methanol synthesis. It is interesting to note that it is the formation of the C-rich biochar co-product in pyrolysis that allows the production of a syngas with a high H:C ratio (approx. 1.4 molar for pyrolysis at 450 °C with tar-cracking at 800 °C). By comparison, gasification of biomass produces a syngas with a H₂:CO ratio so low (< 1) that maximum syngas-C to methanol-C recovery is generally below 50%.⁷⁴



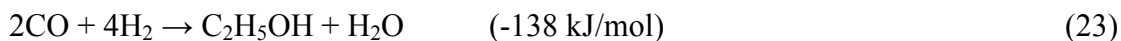
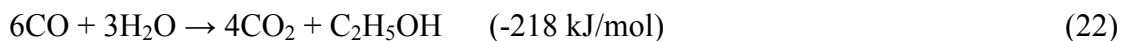
Typical industrial methanol production facilities achieve syngas-C to methanol-C conversion of > 90% (90% was assumed here) with a syngas-to-methanol thermal efficiency of > 90%⁷⁵ C-conversion efficiency for biomass to methanol plants is likely to be at the lower end of this range due to the smaller size expected of biomass facilities, with a C recovery of 90% being assumed here.

2.2.2 Higher alcohols

Longer chain alcohols are often considered to be preferable to methanol for use as transport fuels due to their greater energy density. Of these, ethanol has received the most attention because it is more readily synthesised than propanol or butanol. Currently, bio-ethanol is typically a 1st generation biofuel, produced from sugar or starch crops, such as maize, sugar cane or cassava, which compete for land with food production. Recently, however, there has been a growth in interest in the fermentation of biomass-derived syngas using microbial catalysts that are able to metabolise CO, CO₂ and H₂ (such as *Clostridium jungdahlii*, *Clostridium carboxidivorans*, *Clostridium aceticum*, *Clostridium autoethanogenum*, or *Butyribacterium methylotrophicum*) to produce alcohols as 2nd generation biofuels from lignocellulosic biomass.⁷⁶ Bio-catalysts have some advantages such as high specificity for the desired product, independence of the H₂:CO ratio of the syngas, and operation at ambient conditions. The main challenges facing syngas biocatalysts are (a) the low solubility of CO and H₂, giving rise to poor mass transfer properties, and (b) the low concentration of product in water (up to approximately 4% for ethanol from *C. ljungdahlii*), giving rise to large energy requirements for distillation.⁷⁷ Use of reactor configurations such as air-lift reactors, micro-sparger columns or continuously stirred reactors can alleviate mass transfer issues.⁷⁸ Integration of heat requirements for distillation with waste

heat from syngas production can alleviate the second of these issues. Demonstration-scale industrial facilities using *C. Ljungdahlii* have already been built by companies such as *Coskata*⁷⁹ and *Ineos Bio*⁸⁰.

Metabolism of CO to ethanol follows the Ljungdahl-Wood pathway.⁸¹ In the absence of H₂, the overall reaction stoichiometry is as shown in Eq. 22, which yields a maximum C recovery of 33% in the ethanol product. When both CO and H₂ are available, however, *theoretical* C recoveries of up to 100% are possible for a H₂:CO ratio of 2:1, according to Eq. 23.



Assuming that available H₂ is utilised in Eq. 23 and that any surplus CO is utilised by Eq. 22, the maximum C recovery (R_C) possible can thus be expressed as a function of H₂:CO as in Eq. 24.

$$R_C = \begin{cases} \frac{1}{3}(H_2:CO + 1) & , H_2:CO < 2 \\ 1 & , H_2:CO \geq 2 \end{cases} \quad (24)$$

In practice, some syngas-C is also utilised to generate microbial biomass and other metabolic co-products (principally acetate), reducing the C recovery to below the theoretical maximum. Furthermore, mass transfer constraints mean that a fraction of the incoming CO will always remain in the exhaust gas. There is a law of diminishing returns in terms of the size of reactor required and/or quantity of spent-gas recycling required to increase the fraction of incoming CO metabolised by microbes, with the energy and cost required to lower this fraction becoming larger as the CO remaining approaches zero. Actual C recoveries reported range from 85-95% of maximum,⁸²⁻⁸⁴ and 90% was assumed here.

Distillation of ethanol from the broth (water-rich mixture produced by fermentation) represents a significant component of the overall energy balance. In response to both economic pressure and also to criticisms of the poor energy balance of corn ethanol production⁸⁵ the energy use in ethanol production has steadily declined over the last decade. Currently, corn ethanol production in the USA uses on average 0.43 kJ of heating fuel to produce 1 kJ of ethanol.⁸⁶ However, modern corn ethanol facilities produce a broth of 12% (v/v) ethanol,⁸⁷ whereas syngas fermentation can typically yield a broth of up to 4% ethanol (v/v), although concentrations as high as 4.8% have been reported.⁸⁸ The energy required to distill a 4% ethanol broth to near azeotropic is approximately 7.5 MJ kg⁻¹ etOH.⁸⁹ However, the broth derived from syngas fermentation is a ternary mixture that also contains acetic acid, requiring greater energy expenditure for ethanol separation. Taking this factor into consideration, the process heat required to produce and purify ethanol by syngas fermentation has been estimated to be 18.9 MJ kg⁻¹ etOH (0.64 kJ kJ⁻¹ etOH).⁹⁰ It was assumed that energy recovered in cooling the syngas from the tar cracker (which operates at 800 °C) would contribute to this heat requirement.

2.2.3 Fischer-Tropsch alkanes

Fischer–Tropsch (FT) synthesis converts syngas into a range of hydrocarbons in the presence of a catalyst (Eq. 25). The products are predominantly straight-chain alkanes, although smaller quantities of unsaturated hydrocarbons and oxygenated hydrocarbons such as alcohols may also be formed. The prevailing paradigm is that FT systems have very large economies of scale and are currently only used at the large scale (18,000 – 140,000 barrels per day production), poorly compatible with a distributed biomass-to-fuel infrastructure.⁹¹ However, recent developments

such as micro-channel catalysts show strong potential to operate economically at a smaller scale.^{91,92}



FT products cover a wide range of molecular weights from CH₄ to long-chain waxes with $n > 15$. The distribution of molecular weights approximately follows an Anderson–Schulz–Flory (ASF) distribution (Eq. 26, Fig. S6), in which the chain-growth probability, α , is determined by catalyst and process conditions.⁹³ Temperature is a particularly important determinant of α , with higher temperatures yielding a greater fraction of methane (lower α), but also faster reaction kinetics.⁹³

$$W_n = n(1-\alpha)^2\alpha^{n-1}, \quad (26)$$

where W_n is the fraction of product with n C-atoms in a molecule.

In practice, the product distribution typically deviates from the ideal ASF distribution due to secondary reactions of olefins, yielding more C1, less C2 and a more linear distribution of higher hydrocarbons than predicted by ASF.⁹⁴ Notwithstanding these deviations from the ideal, optimising reactor conditions for a low yield of gases (C1 and C2) results in considerable quantities of wax (Fig. S6) which require further hydrocracking and refining to be converted to liquid fuels. In a distributed small-scale biomass energy systems, FT products, including wax, could, in principle, be transported to a centralised refinery for further processing. In most FT systems, yield of gas is typically minimised because liquid fuel is the desired product. However, when biomass pyrolysis rather than gasification is used for the primary conversion to syngas, an alternative system configuration is feasible that would preclude the need for a centralised refinery. In a pyrolysis-FT system, the FT gas products could be recycled to provide heat for pyrolysis and tar-cracking, thus allowing the FT process to be optimised for a greater production of gas and liquid fuels while minimising wax production and thus removing the requirement for further downstream hydrocracking.

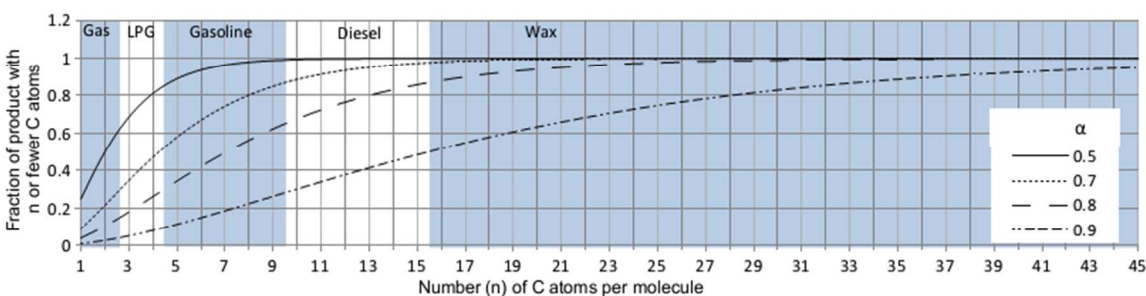


Fig. S6: Theoretical cumulative distribution of products from Fischer-Tropsch synthesis follows the Anderson–Schulz–Flory distribution (Eq. 26), shown here for values of α (the chain-growth probability) from 0.5 to 0.9.

A high-temperature FT system of this type was modelled by assuming that the products follow the ASF distribution, with α set such that the gaseous products (including unreacted syngas) would be just sufficient to provide process heat and power for pyrolysis and tar-cracking (assuming a gas-to-heat thermal efficiency of 80%), except where this would imply $\alpha > 0.9$, in which case α was assumed to be 0.9. , CO conversion was assumed to be 70%, as achievable with a once-through micro-channel reactor suited to small-scale operation.⁹²

2.2.4 Bio-oils

The term 'bio-oil' is used here to refer to the entire spectrum of volatile organic compounds produced in pyrolysis. Most recent research and development of pyrogenic bio-oil fuels has focussed on fast-pyrolysis with its higher yield of oil than slow pyrolysis.^{95,96} Fast pyrolysis can give liquid yields of up to 80%,^{2,95} although a 75% yield containing 70% of the biomass energy value, together with a biochar yield of 13%, is more typical.⁹⁷

Bio-oils are complex mixtures containing dozens to potentially hundreds of compounds, their compositions being highly variable depending on feedstock composition, size and moisture content and on pyrolysis conditions.^{30,37,98-100} Typical composition includes organic acids, esters, alcohols, ketones, aldehydes, sugars, furans, phenols, guaiacols, syringols and miscellaneous oxygenated organic compounds such as glycolaldehyde and acetol in widely varying abundances.⁹⁸ Without upgrading, bio-oils are poorly suited to use as fuel. Their high oxygen content (35-40% O) gives rise to a low heating value (HHV=16-19 GJ/Mg); high water content (15-30%) also contributes to a low HHV and can give rise to phase separation; a low pH (2-3) can corrode pipes and engine components; suspended solids (char and ash) can also erode engine components or cause blockages, with alkali metals in ash being particularly damaging to engines and turbines; also, bio-oils are generally chemically unstable and may degrade further in storage.^{96,101} The two methods most often suggested for upgrading of pyrolysis oils are hydro-deoxygenation (removal of oxygen by reaction with hydrogen) or zeolite catalysis.^{96,101} The high cost of providing hydrogen is often the limiting factor in application of hydro-deoxygenation. Also, little research has been undertaken to ascertain the suitability of slow pyrolysis oils for upgrading to transport fuels. Therefore, the current study does not include slow pyrolysis oils. Bio-oils from fast pyrolysis, which have been more studied, are used here as a point of reference to compare to the other slow-pyrolysis derived fuels described above.

It is becoming established practice in industrial fast pyrolysis systems to utilise the solid product to supply process energy for both the pyrolysis itself and for fuel upgrading. If the solids are to be used as a biochar soil amendment instead, an alternative source of process energy would be required. It was assumed that this process energy would be supplied by an amount of bio-oil with energy content equivalent to the biochar that would otherwise have been utilised for energy. Thus, for a 13% yield of biochar with C content of 80% (i.e. a biochar C yield of 0.10 Mg C Mg⁻¹ DM), and with a HHV of 30 GJ Mg⁻¹,² this implies that 3.9 GJ bio-oil Mg⁻¹ feedstock would be required to provide process heat (if the biochar were used for soil application). Assuming that 14 GJ Mg⁻¹ DM bio-oil is produced when biochar combustion contributes to the process heat requirements,⁹⁷ then 10.1 GJ could be available after a fraction of the bio-oil has been used for process energy. To treat fast pyrolysis equivalently to the calculations for slow pyrolysis, we also need to assume that the parasitic power consumption (0.75 GJe Mg⁻¹ DM,⁹⁷) would be generated from bio-oil at a thermal efficiency of 30%, giving a net energy production per Mg of dry feedstock of 11.5 GJ if the biochar is utilised for energy or 7.6 GJ if the biochar is used as a soil amendment.

Table S3: Summary of chemical reactions for the conversion pathways from syngas to biofuels.

Reaction	ΔH° (kJ mol ⁻¹) ^a
<u>Water gas shift:</u>	
$\text{CO} + \text{H}_2\text{O} \rightarrow \text{CO}_2 + \text{H}_2$	-41
<u>Catalytic methanation:</u>	
$\text{CO} + 3\text{H}_2 \rightarrow \underline{\text{CH}_4} + \text{H}_2\text{O}$	-206
$2\text{CO} + 2\text{H}_2 \rightarrow \underline{\text{CH}_4} + \text{CO}_2$	-247
$\text{CO}_2 + 4\text{H}_2 \rightarrow \underline{\text{CH}_4} + 2\text{H}_2\text{O}$	-165
<u>Methanol synthesis:</u>	
$\text{CO} + 2\text{H}_2 \rightarrow \underline{\text{CH}_3\text{OH}}$	-91
$\text{CO}_2 + 3\text{H}_2 \rightarrow \underline{\text{CH}_3\text{OH}} + \text{H}_2\text{O}$	-49
<u>Ljungdahl-Wood pathway:</u>	
$6\text{CO} + 3\text{H}_2\text{O} \rightarrow 4\text{CO}_2 + \underline{\text{C}_2\text{H}_5\text{OH}}$	-218
$2\text{CO} + 4\text{H}_2 \rightarrow \underline{\text{C}_2\text{H}_5\text{OH}} + \text{H}_2\text{O}$	-138
<u>Fischer-Tropsch synthesis:</u>	
$n\text{CO} + (2n+1)\text{H}_2 \rightarrow \underline{\text{C}_n\text{H}_{(2n+2)}} + n\text{H}_2\text{O}$	

^a ΔH° is expressed per mole of the biofuel product (underlined).

References

- (1) Thunman, H.; Niklasson, F.; Johnsson, F.; Leckner, B. Composition of Volatile Gases and Thermochemical Properties of Wood for Modeling of Fixed or Fluidized Beds. *Energy Fuels* **2001**, *15*, 1488–1497.
- (2) Neves, D.; Thunman, H.; Matos, A.; Tarelho, L.; Gómez-Barea, A. Characterization and prediction of biomass pyrolysis products. *Progress in Energy and Combustion Science* **2011**, *37*, 611–630.
- (3) Roberts, K. G.; Gloy, B. A.; Joseph, S.; Scott, N. R.; Lehmann, J. Life Cycle Assessment of Biochar Systems: Estimating the Energetic, Economic, and Climate Change Potential. *Environmental Science & Technology* **2010**.
- (4) Brown, T. R.; Wright, M. M.; Brown, R. C. Estimating profitability of two biochar production scenarios: slow pyrolysis vs fast pyrolysis. *Biofuels, Bioproducts and Biorefining* **2011**, *5*, 54–68.
- (5) Field, J. L.; Keske, C. M. H.; Birch, G. L.; DeFoort, M. W.; Cotrufo, M. F. Distributed biochar and bioenergy coproduction: a regionally specific case study of environmental benefits and economic impacts. *GCB Bioenergy* **2013**, *5*, 177–191.
- (6) Shackley, S.; Hammond, J.; Gaunt, J.; Ibarrola, R. The feasibility and costs of biochar deployment in the UK. *Carbon* **2011**, *2*, 335–356.
- (7) Hammond, J.; Shackley, S.; Sohi, S.; Brownsort, P. Prospective life cycle carbon abatement for pyrolysis biochar systems in the UK. *Energy Policy* **2011**, *39*, 2646–2655.
- (8) Wang, Z.; Dunn, J. B.; Han, J.; Wang, M. Q. Effects of co-produced biochar on life cycle greenhouse gas emissions of pyrolysis-derived renewable fuels. *Biofuels, Bioprod. Bioref.* **2014**, *8*, 189–204.
- (9) Encinar, J. .; González, J. .; González, J. Fixed-bed pyrolysis of *Cynara cardunculus* L. Product yields and compositions. *Fuel Processing Technology* **2000**, *68*, 209–222.
- (10) Fagbemi, L.; Khezami, L.; Capart, R. Pyrolysis products from different biomasses: application to the thermal cracking of tar. *Applied Energy* **2001**, *69*, 293–306.
- (11) Di Blasi, C.; Signorelli, G.; Di Russo, C.; Rea, G. Product distribution from pyrolysis of wood and agricultural residues. *Ind. Eng. Chem. Res.* **1999**, *38*, 2216–2224.
- (12) Becidan, M.; Skreiberg, Ø.; Hustad, J. E. Products distribution and gas release in pyrolysis of thermally thick biomass residues samples. *Journal of Analytical and Applied Pyrolysis* **2007**, *78*, 207–213.
- (13) Bassilakis, R.; Carangelo, R. .; Wójtowicz, M. . TG-FTIR analysis of biomass pyrolysis. *Fuel* **2001**, *80*, 1765–1786.
- (14) De Wild, P. J.; Uil, H. den; Reith, J. H.; Kiel, J. H. A.; Heeres, H. J. Biomass valorisation by staged degasification: A new pyrolysis-based thermochemical conversion option to produce value-added chemicals from lignocellulosic biomass. *Journal of Analytical and Applied Pyrolysis* **2009**, *85*, 124–133.
- (15) Bennadji, H.; Smith, K.; Shabangu, S.; Fisher, E. M. Low-Temperature Pyrolysis of Woody Biomass in the Thermally Thick Regime. *Energy Fuels* **2013**, *27*, 1453–1459.
- (16) Gauthier, G.; Melkior, T.; Grateau, M.; Thiery, S.; Salvador, S. Pyrolysis of centimetre-scale wood particles: New experimental developments and results. *Journal of Analytical and Applied Pyrolysis* **2013**, *In Press*.
- (17) Di Blasi, C. Modeling chemical and physical processes of wood and biomass pyrolysis. *Progress in Energy and Combustion Science* **2008**, *34*, 47–90.
- (18) Demirbas, A. Carbonization ranking of selected biomass for charcoal, liquid and gaseous products. *Energy Conversion and Management* **2001**, *42*, 1229–1238.

- (19) Karaosmanoglu, F.; Tetik, E.; Göllü, E. Biofuel production using slow pyrolysis of the straw and stalk of the rapeseed plant. *Fuel Processing Technology* **1999**, *59*, 1–12.
- (20) Williams, P. T.; Besler, S. The influence of temperature and heating rate on the slow pyrolysis of biomass. *Renew Energ.* **1996**, *7*, 233–250.
- (21) Beis, S. H.; Onay, Ö.; Koçkar, Ö. M. Fixed-bed pyrolysis of safflower seed: influence of pyrolysis parameters on product yields and compositions. *Renewable Energy* **2002**, *26*, 21–32.
- (22) Şensöz, S.; Demiral, İ.; Ferdi Gerçel, H. Olive bagasse (*Olea europea* L.) pyrolysis. *Bioresource Technology* **2006**, *97*, 429–436.
- (23) Raveendran, K.; Ganesh, A.; Khilar, K. C. Pyrolysis characteristics of biomass and biomass components. *Fuel* **1996**, *75*, 987–998.
- (24) Apaydin-Varol, E.; Pütün, E.; Pütün, A. E. Slow pyrolysis of pistachio shell. *Fuel* **2007**, *86*, 1892–1899.
- (25) Zandersons, J.; Gravitis, J.; Kokorevics, A.; Zhurinsh, A.; Bikovens, O.; Tardenaka, A.; Spince, B. Studies of the Brazilian sugarcane bagasse carbonisation process and products properties. *Biomass Bioenerg.* **1999**, *17*, 209–219.
- (26) Schröder, E. Experiments on the pyrolysis of large beechwood particles in fixed beds. *Journal of Analytical and Applied Pyrolysis* **2004**, *71*, 669–694.
- (27) Demirbaş, A. Properties of charcoal derived from hazelnut shell and the production of briquettes using pyrolytic oil. *Energy* **1999**, *24*, 141–150.
- (28) Şensöz, S.; Angin, D. Pyrolysis of safflower (*Charthamus tinctorius* L.) seed press cake: Part 1. The effects of pyrolysis parameters on the product yields. *Bioresource Technology* **2008**, *99*, 5492–5497.
- (29) Şensöz, S.; Can, M. Pyrolysis of Pine (*Pinus Brutia* Ten.) Chips: 1. Effect of Pyrolysis Temperature and Heating Rate on the Product Yields. *Energy Sources* **2002**, *24*, 347–355.
- (30) Özbay, N.; Pütün, A. .; Uzun, B. .; Pütün, E. Biocrude from biomass: pyrolysis of cottonseed cake. *Renewable Energy* **2001**, *24*, 615–625.
- (31) Pütün, A. E.; Önal, E.; Uzun, B. B.; Özbay, N. Comparison between the “slow” and “fast” pyrolysis of tobacco residue. *Industrial Crops and Products* **2007**, *26*, 307–314.
- (32) Pütün, A. .; Özcan, A.; Pütün, E. Pyrolysis of hazelnut shells in a fixed-bed tubular reactor: yields and structural analysis of bio-oil. *Journal of Analytical and Applied Pyrolysis* **1999**, *52*, 33–49.
- (33) ECN. Phyllis, database for biomass and waste. **2012**.
- (34) Yang, H.; Yan, R.; Chen, H.; Zheng, C.; Lee, D. H.; Liang, D. T. In-Depth Investigation of Biomass Pyrolysis Based on Three Major Components: □ Hemicellulose, Cellulose and Lignin. *Energy & Fuels* **2006**, *20*, 388–393.
- (35) Yang, H.; Yan, R.; Chen, H.; Lee, D. H.; Zheng, C. Characteristics of hemicellulose, cellulose and lignin pyrolysis. *Fuel* **2007**, *86*, 1781–1788.
- (36) Fahmi, R.; Bridgwater, A. V.; Donnison, I.; Yates, N.; Jones, J. M. The effect of lignin and inorganic species in biomass on pyrolysis oil yields, quality and stability. *Fuel* **2008**, *87*, 1230–1240.
- (37) Agblevor, F.; Besler-Guran, S.; Montane, D.; Wiselogel, A. Biomass feedstock variability and its effect on biocrude oil properties. In *Developments in thermochemical biomass conversion*, Bridgwater, A. and Boocock, D. (Eds); Springer, 1997; pp. 741–755.
- (38) Scott, D. S.; Majerski, P.; Piskorz, J.; Radlein, D. A second look at fast pyrolysis of biomass—the RTI process. *Journal of Analytical and Applied Pyrolysis* **1999**, *51*, 23–37.
- (39) Figueiredo, J. L.; Valenzuela, C.; Bernalte, A.; Encinar, J. M. Pyrolysis of holm-oak wood: influence of temperature and particle size. *Fuel* **1989**, *68*, 1012–1016.

- (40) Encinar, J. M.; Beltran, F. J.; Bernalte, A.; Ramiro, A.; Gonzalez, J. F. Pyrolysis of two agricultural residues: olive and grape bagasse. Influence of particle size and temperature. *Biomass and Bioenergy* **1996**, *11*, 397–409.
- (41) Demirbas, A. Effects of temperature and particle size on bio-char yield from pyrolysis of agricultural residues. *J. Anal. Appl. Pyrol.* **2004**, *72*, 243–248.
- (42) Valenzuela-Calahorra, C.; Bernalte-Garcia, A.; Gómez-Serrano, V.; Bernalte-García, M. J. Influence of particle size and pyrolysis conditions on yield, density and some textural parameters of chars prepared from holm-oak wood. *Journal of Analytical and Applied Pyrolysis* **1987**, *12*, 61–70.
- (43) Şensöz, S.; Angin, D.; Yorgun, S. Influence of particle size on the pyrolysis of rapeseed (< i> Brassica napus</i> L.): fuel properties of bio-oil. *Biomass and Bioenergy* **2000**, *19*, 271–279.
- (44) Chan, W. C. .; Kelbon, M.; Krieger-Brockett, B. Single-particle biomass pyrolysis: correlations of reaction products with process conditions. *Industrial & engineering chemistry research* **1988**, *27*, 2261–2275.
- (45) Demirbas, A. Effect of initial moisture content on the yields of oily products from pyrolysis of biomass. *Journal of analytical and applied pyrolysis* **2004**, *71*, 803–815.
- (46) Mok, W. S.-L.; Antal Jr., M. J. Effects of pressure on biomass pyrolysis. II. Heats of reaction of cellulose pyrolysis. *Thermochimica Acta* **1983**, *68*, 165–186.
- (47) Antal, M.; Grønli, M. The Art, Science, and Technology of Charcoal Production. *Ind. Eng. Chem. Res* **2003**, *42*, 1619–1640.
- (48) Sensöz, S. Slow pyrolysis of wood barks from Pinus brutia Ten. and product compositions. *Bioresource Technology* **2003**, *89*, 307–311.
- (49) NASA. *Chemical Equilibrium with Applications (CEA)*; <http://www.grc.nasa.gov/WWW/CEAWeb/>, 2004.
- (50) Channiwala, S. A.; Parikh, P. P. A unified correlation for estimating HHV of solid, liquid and gaseous fuels. *Fuel* **2002**, *81*, 1051–1063.
- (51) Pyle, D. L.; Zaror, C. A. Heat transfer and kinetics in the low temperature pyrolysis of solids. *Chemical Engineering Science* **1984**, *39*, 147–158.
- (52) Di Blasi, C. Kinetic and Heat Transfer Control in the Slow and Flash Pyrolysis of Solids. *Ind. Eng. Chem. Res.* **1996**, *35*, 37–46.
- (53) <http://webbook.nist.gov>. Water (accessed Jun 13, 2013).
- (54) Rabou, L. P. L. M.; Zwart, R. W. R.; Vreugdenhil, B. J.; Bos, L. Tar in Biomass Producer Gas, the Energy research Centre of The Netherlands (ECN) Experience: An Enduring Challenge. *Energy Fuels* **2009**, *23*, 6189–6198.
- (55) www.engineeringtoolbox.com. Gases - Specific Heats and Individual Gas Constants (accessed Oct 13, 2012).
- (56) Luo, Z.; Wang, S.; Cen, K. A model of wood flash pyrolysis in fluidized bed reactor. *Renewable Energy* **2005**, *30*, 377–392.
- (57) Lu, Q.; Yang, X.; Zhu, X. Analysis on chemical and physical properties of bio-oil pyrolyzed from rice husk. *Journal of Analytical and Applied Pyrolysis* **2008**, *82*, 191–198.
- (58) Bridgwater, A. V.; Toft, A. J.; Brammer, J. G. A techno-economic comparison of power production by biomass fast pyrolysis with gasification and combustion. *Renewable and Sustainable Energy Reviews* **2002**, *6*, 181–246.
- (59) Thomsen, T.; Hauggaard-Nielsen, H.; Bruun, E.; Ahrenfeldt, J. *The potential of Pyrolysis Technology in climate change mitigation: Influence of process design and parameters, simulated in SuperPro Designer Software*; Risø-R-1764 (EN); Risø National Laboratory for Sustainable Energy, 2011.

- (60) Mälkki, H.; Virtanen, Y. Selected emissions and efficiencies of energy systems based on logging and sawmill residues. *Biomass and Bioenergy* **2003**, *24*, 321–327.
- (61) Crabtree, G. W.; Dresselhaus, M. S.; Buchanan, M. V. The hydrogen economy. *Physics Today* **2004**, *57*, 39.
- (62) Olah, G. A. Beyond Oil and Gas: The Methanol Economy. *Angewandte Chemie International Edition* **2005**, *44*, 2636–2639.
- (63) Berglund, M.; Börjesson, P. Assessment of energy performance in the life-cycle of biogas production. *Biomass and Bioenergy* **2006**, *30*, 254–266.
- (64) Lastella, G.; Testa, C.; Cornacchia, G.; Notornicola, M.; Voltasio, F.; Sharma, V. K. Anaerobic digestion of semi-solid organic waste: biogas production and its purification. *Energy Conversion and Management* **2002**, *43*, 63–75.
- (65) Petersson, A.; WeLLInGer, A. Biogas upgrading technologies—developments and innovations. *IEA-Task* **2009**, *37*, 20.
- (66) Weiland, P. Production and energetic use of biogas from energy crops and wastes in Germany. *Applied biochemistry and biotechnology* **2003**, *109*, 263–274.
- (67) Pöschl, M.; Ward, S.; Owende, P. Evaluation of energy efficiency of various biogas production and utilization pathways. *Applied Energy* **2010**, *87*, 3305–3321.
- (68) Watson, G. H. *Methanation catalysts*; ICTIS/TR09; IEA Coal Research: London, 1980.
- (69) Kopyscinski, J.; Schildhauer, T. J.; Biollaz, S. M. A. Production of synthetic natural gas (SNG) from coal and dry biomass – A technology review from 1950 to 2009. *Fuel* **2010**, *89*, 1763–1783.
- (70) Van der Meijden, C. M.; Veringa, H. J.; Rabou, L. P. L. M. The production of synthetic natural gas (SNG): A comparison of three wood gasification systems for energy balance and overall efficiency. *Biomass and Bioenergy* **2010**, *34*, 302–311.
- (71) Olah, G. A.; Prakash, G. K. S.; Goepfert, A. Anthropogenic chemical carbon cycle for a sustainable future. *Journal of the American Chemical Society* **2011**.
- (72) Güllü, D.; Demirbaş, A. Biomass to methanol via pyrolysis process. *Energy Conversion and Management* **2001**, *42*, 1349–1356.
- (73) Radovic, L. R.; Vannice, M. A. Sulfur tolerance of methanol synthesis catalysts: Modelling of catalyst deactivation. *Applied Catalysis* **1987**, *29*, 1–20.
- (74) Mathieu, P.; Dubuisson, R. Performance analysis of a biomass gasifier. *Energy Conversion and Management* **2002**, *43*, 1291–1299.
- (75) Bain, R. L. *Material and Energy Balances for Methanol from Biomass Using Biomass Gasifiers*; NREL/TP-510-17098; National Renewable Energy Laboratory, 1992.
- (76) Henstra, A. M.; Sipma, J.; Rinzema, A.; Stams, A. J. Microbiology of synthesis gas fermentation for biofuel production. *Current Opinion in Biotechnology* **2007**, *18*, 200–206.
- (77) Munasinghe, P. C.; Khanal, S. K. Biomass-derived syngas fermentation into biofuels: Opportunities and challenges. *Bioresource Technology* **2010**, *101*, 5013–5022.
- (78) Munasinghe, P. C.; Khanal, S. K. Syngas fermentation to biofuel: Evaluation of carbon monoxide mass transfer coefficient (kLa) in different reactor configurations. *Biotechnol Progress* **2010**, n/a–n/a.
- (79) Coskata. Coskata, Inc. <http://www.coskata.com/> (accessed Oct 2, 2012).
- (80) INEOS Bio. Welcome to INEOS Bio - Ineos Bio - Renewable Bioenergy http://www.ineosbio.com/57-Welcome_to_INEOS_Bio.htm (accessed Oct 2, 2012).
- (81) Ragsdale, S. W.; Wood, H. G. Enzymology of the Acetyl-CoA Pathway of CO₂ Fixation. *Critical Reviews in Biochemistry and Molecular Biology* **1991**, *26*, 261–300. 2
- (82) Mohammadi, M.; Younesi, H.; Najafpour, G.; Mohamed, A. R. Sustainable ethanol fermentation from synthesis gas by *Clostridium ljungdahlii* in a continuous stirred tank bioreactor. *Journal of Chemical Technology & Biotechnology* **2012**, *87*, 837–843.

- (83) Rajagopalan, S.; P. Datar, R.; Lewis, R. S. Formation of ethanol from carbon monoxide via a new microbial catalyst. *Biomass and Bioenergy* **2002**, *23*, 487–493.
- (84) Sakai, S.; Nakashimada, Y.; Yoshimoto, H.; Watanabe, S.; Okada, H.; Nishio, N. Ethanol production from H₂ and CO by a newly isolated thermophilic bacterium. *Biotechnology Letters* **2004**, *26*, 1607–1612.
- (85) Pimentel, D. Ethanol Fuels: Energy Balance, Economics, and Environmental Impacts Are Negative. *Natural Resources Research* **2003**, *12*, 127–134.
- (86) Gallagher, P. W.; Shapouri, H. Improving Sustainability of the Corn-Ethanol Industry. In *Biofuels*; John Wiley & Sons, Ltd, 2009; pp. 223–234.
- (87) Bai, F. W.; Anderson, W. A.; Moo-Young, M. Ethanol fermentation technologies from sugar and starch feedstocks. *Biotechnology Advances* **2008**, *26*, 89–105.
- (88) Klasson, K. T.; Ackerson, M. D.; Clausen, E. C.; Gaddy, J. L. Biological conversion of coal and coal-derived synthesis gas. *Fuel* **1993**, *72*, 1673–1678.
- (89) Vane, L. M. Separation technologies for the recovery and dehydration of alcohols from fermentation broths. *Biofuels, Bioproducts and Biorefining* **2008**, *2*, 553–588.
- (90) Piccolo, C.; Bezzo, F. A techno-economic comparison between two technologies for bioethanol production from lignocellulose. *Biomass and Bioenergy* **2009**, *33*, 478–491.
- (91) Atkinson, D. Fischer-Tropsch reactors for biofuels production: new technology needed! *Biofuels, Bioproducts and Biorefining* **2010**, *4*, 12–16.
- (92) Deshmukh, S. R.; Tonkovich, A. L. Y.; Jarosch, K. T.; Schrader, L.; Fitzgerald, S. P.; Kilanowski, D. R.; Lerou, J. J.; Mazanec, T. J. Scale-Up of Microchannel Reactors For Fischer–Tropsch Synthesis. *Ind. Eng. Chem. Res.* **2010**, *49*, 10883–10888.
- (93) Dry, M. E. The Fischer–Tropsch process: 1950–2000. *Catalysis Today* **2002**, *71*, 227–241.
- (94) Schulz, H.; Claeys, M. Kinetic modelling of Fischer–Tropsch product distributions. *Applied Catalysis A: General* **1999**, *186*, 91–107.
- (95) Bridgwater, A. V.; Cottam, M. L. Opportunities for biomass pyrolysis liquids production and upgrading. *Energy Fuels* **1992**, *6*, 113–120.
- (96) Mohan, D.; Pittman; Steele, P. H. Pyrolysis of Wood/Biomass for Bio-oil: □ A Critical Review. *Energy & Fuels* **2006**, *20*, 848–889.
- (97) Bridgwater, A. V. *Technical and Economic Assessment of Thermal Processes for Biofuels*; 2009.
- (98) Branca, C.; Giudicianni, P.; Di Blasi, C. GC/MS Characterization of Liquids Generated from Low-Temperature Pyrolysis of Wood. *Ind. Eng. Chem. Res.* **2003**, *42*, 3190–3202.
- (99) Di Blasi, C.; Branca, C. Kinetics of Primary Product Formation from Wood Pyrolysis. *Ind. Eng. Chem. Res.* **2001**, *40*, 5547–5556.
- (100) Ranzi, E.; Cuoci, A.; Faravelli, T.; Frassoldati, A.; Migliavacca, G.; Pierucci, S.; Sommariva, S. Chemical Kinetics of Biomass Pyrolysis. *Energy Fuels* **2008**, *22*, 4292–4300.
- (101) Huber, G. W.; Iborra, S.; Corma, A. Synthesis of Transportation Fuels from Biomass: □ Chemistry, Catalysts, and Engineering. *Chem. Rev.* **2006**, *106*, 4044–4098.